

# New Evaluation Techniques of Hyperspectral Data

Veronika KOZMA-BOGNÁR  
Georgikon Faculty, University of Pannonia  
Keszthely, H-8360, Hungary

and

József BERKE  
Basic and Technical Sciences Institute, Dennis Gabor Applied University  
Budapest, H-1119, Hungary

## ABSTRACT

Multiband aerial imagery in remote sensing is a technology used more and more widely in present days. It can excellently be used in research fields where there is need for high spectral resolution images in order to obtain adequate level results. At present, data collection is of a much higher level than processing and use. As the technical development of sensors is followed by a significant delay in data processing methods and applications, it seems reasonable to refine processing methods as well as to widen practical uses (agriculture, environmental protection).

In the year of 2004, a new examination method based on fractal structure was introduced, which, according to our experiences, has made more accurate spectral measurement possible as opposed to other techniques. The mathematical process named spectral fractal dimension (SFD) is directly applicable in multi-dimension colour space as well, making thus possible to choose new examination methods of multiband images. With the help of SFD, it is possible to obtain more useful data offered by high spectral resolution, or to choose the bands wished to process applying different methods later.

**Keywords:** remote sensing, image processing, hyperspectral images, REIP, SFD.

## 1. INTRODUCTION

Remote sensing images can be classified according to several points, eg. the aim of data collection, the height of where the image was taken, spatial resolution, wave length range, or the number of channels. Based on the number of channels, the following classes can be identified:

Panchromatic images: 1 channel  
Colour images: 3 channels  
Multispectral images: 4-20 channels  
Hyperspectral images: 21- channels [5]

Panchromatic images are usually of high spatial resolution, and are made integrating visible and near infrared range. Multispectral images contain several channels of wider band channels, whereas hyperspectral images are of narrow band width (0,01  $\mu\text{m}$ ) with greater number of channels [12, 14]. In images taken in more than one channels-due to high spectral resolution-, landmarks and surface details can more easily be identified than using only one channel. That is the reason why the application of multispectral and hyperspectral imagery devices is getting more and more emphasis nowadays.

Remote sensing applies and records electromagnetic energy reflected or emitted by the objects on the soil surface. Detecting devices primarily detect reflected energy with wavelengths under 3000 nm, whereas with wavelengths over 5000 nm, emitted energy is detected. Elements of different characteristics will take a different reflection (or emission) value in certain wavelength ranges, depending on the physical and electromagnetic features, as well as the wavelength of the electromagnetic radiation of a given substance. The curve of reflection values of objects represented in a wavelength graph is called a spectral reflection curve [12]. Based on this curve, microorganisms, minerals, plants, buildings and artificial materials can easily be identified, as different materials have different reflection curves due to their different characteristics. Digital spectral libraries (USGS Digital Spectral Library, Aster Spectral Library), containing 'spectral fingerprints' recorded under given conditions and collected in libraries, play a significant role in spectral identification. The standard spectral profiles are usually used as references in the identification of elements.

In the scientific literature on surface reflectance, several indexes can be found that are generated from the reflection curve values and certain differences. NDVI (Normalised Difference Vegetation Index) is a vegetation index that is a first generation index widely spread in remote sensing showing photosynthetically active vegetation. In case the examined plant file contains soil spots as well, then SAVI (Soil-Adjusted Vegetation Index) is to be used. Red Edge Index is considered to be a second generation - or, after Broge and Mortensen [3], a new generation - index, which describes the shape and relative situation of the reflection curve (Red Edge Inflection Point - REIP). Throughout the evaluation of the curve, the health state, stress toleration ability, chlorophyll content, and infection level of plants etc. can be judged from the shift of the inflection point [15] Out of several, two relatively simple calculation methods have been used in practice:

Calculating REIP according to Clevers et al. [4]:

$$\lambda_{re} = 700 + (740-700) [(R_{re} - R_{700}) / (R_{740} - R_{700})],$$

where  $R_{re} = (R_{670} + R_{780}) / 2$  (I)

Calculating REIP according to Mutanga-Skidmore [10]:

$$\lambda_{re} = 695 + (742-695) [(R_{re} - R_{695}) / (R_{742} - R_{695})],$$

where  $R_{re} = (R_{663} + R_{788}) / 2$  (II)

where  $R_{re}$  = reflectance of inflection point,  
 $R_{\lambda}$  = reflectance at  $\lambda$  wavelength.

In multi-band imagery technologies, data are recorded in the form of a 'data square', each band of which is an image of the examined area. The intensity values read from the vertical values of image elements of the same area give the steady distribution spectrum of the surface material of the area. The data recorded by multispectral and hyperspectral sensors are raw figures that can be turned into reflectance values having acquired spectroradiometric references later on the spot and other corrections (eg. atmospheric). Reflectance data gained this way take into account the continuously measured reflectance of incoming sunshine as well. After this correction, the recorded spectrum of the image is suitable for comparison to other eg. laboratory spectra. In digital spectrum libraries, data defined under laboratory circumstances are collected, in which no effects of natural phenomena are included. They usually include the data of pure or mixed materials, whereas our remote sensing devices integrate a lot of other unique information in their output data depending on the sensor and atmospheric characteristics, which can significantly differ from one another. In order to acquire more accurate reference data, often on-the-spot spectrometers are used with the use of which differences between sensors can partly be compensated (applying the same series of sensors), though the atmospheric effect can not. A further problem is that the accuracy of on-the-spot spectroscopic examinations is also influenced by several factors (eg. calibration, viewing angle, type of sensor, weather conditions), which can not be post-corrected or repeated.

## 2. MATERIALS AND METHODS

The location of our examinations was 15 km from Keszthely, Hungary, a test area near Várköly, Hungary, where there are several agricultural fields. We have been taking multispectral and hyperspectral aerial images of the scene since 2006. The first hyperspectral images were taken in 2007, using an AISA Dual hyperspectral sensor, which is one of the most significant systems of the European Union. Most important features of the sensors can be seen in Table 1.

**Table 1.** Technical parameters of AISA Dual

	VNIR sensor	SWIR sensor (Hawk)	AISA Dual
<b>Spectral range</b>	400-970 nm	970-2450 nm	400-2450 nm
<b>Spectral channels</b>	244	254	498
<b>Spectral band width</b>	2.3 nm	5.8 nm	
<b>Spectral depth (bit)</b>	12	14	14
<b>Spatial pixel number</b>	1024	320	320
<b>Optics</b>	18.5 mm	22.5 (or 14)	18.04
<b>Image creation speed</b>	Up to 100 image/s	Up to 100 image/s	Up to 100 image/s

AISA Dual, as member of the AISA camera series developed by SPECIM, Finland, was set up by joining AISA Eagle and AISA Hawk sensors in a dual carrier. The two sensors are capable of collecting data synchronically of the same earth band in the 400-2450 nm spectral range, in maximum 498 bands.

In the region of Keszthely, Hungary, there have been flights two times. On 21. May 2007, after the test area of Várköly, the Valley of the River Zala and several parts of the Little Balaton were captured (GPS: Latitude: 46°51'29.82"N, Longitude: 17°17'57.48"E, Google Earth kmz file - [13]). On 19. June 2007, the Várköly area was monitored. The sensor acquired data from a height of nearly 1200 m. The result was images of 1m/pixel resolution in 359 spectral bands. Owing to high channel number, several bands were found that contained different kinds of noise. Based on visual interpretation, three different noise types were identified: geometric, sensor-caused, atmospheric.

Figure 1 shows an AISA image with no noise (254 bands), whereas Figure 2 shows a band with atmospheric noise (273 bands) after geometric and radiometric corrections carried out with the help of a special software named Caligeo (Specim Spectral Imaging Ltd.). In the noiseless images taken on 19. 06. 2007, land usage, agricultural methods can well be identified, borders of fields and agricultural directions can well be distinguished. Detailed information is obtained on the spectral features of the surface, although the resolution does not achieve sub-meter accuracy.

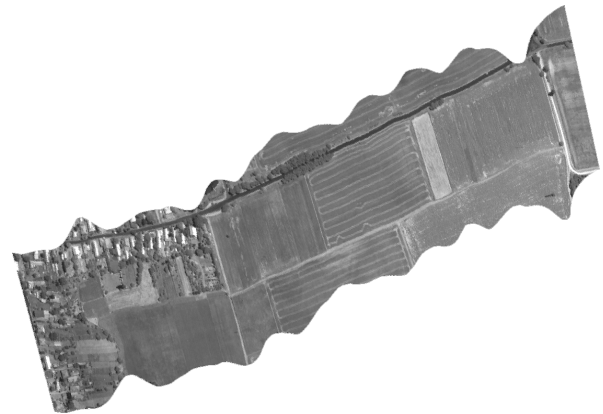


**Figure 1.** Noiseless AISA image of Várköly - 254th band



**Figure 2.** Noisy AISA image of Várköly - 273rd band

Adequate results can also be achieved if we need high terrain resolution but not several channels, or in the lack of financial background to use this equipment, with the application of handheld cameras attached to an aeroplane. Multispectral images were taken of the Várköly test area which achieved sub-meter terrain resolution (10-30 cm). Applied digital devices: Canon EOS digital camera for visible light range (400-

700 nm), Canon EOS digital camera for near infrared range (720-1150 nm), and a thermal infrared (12 000 nm) camera developed by Hexium Company. The images taken by the cameras were georeferenced, thus they became suitable for adequately exact measurements as well as analysis (Fig 3.) [6, 8].

Terrain reference data were acquired at the time of the flight or shortly afterwards. Our primary aim was to map the plant cultures of the area, and we identified several types of vegetation. During later flights, changes were also recorded. The following material and data were collected:

- GPS data,
- meteorological data,
- colour temperature data,
- sample soil data.

The obtained data were recorded in a protocol each time, and the images taken by handheld cameras throughout our work were also enclosed.

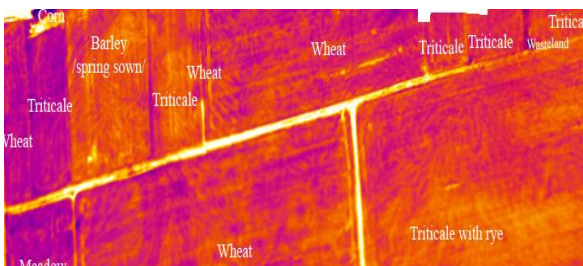


**Figure 3.** Matched and georeferenced aerial images in the visible (A), near (B) and far infrared (C) range, respectively, of the Várköly test area in Zala County, Hungary (photos taken on 19 June, 2007).

When starting the spectral fractal dimension measurement of the different vegetations, we started off the multispectral and hyperspectral images of Várköly and their characteristic reference data. SFD [13] is a structure examining process derived from general fractal dimension [9, 11]. Not only is it suitable for measuring spatial structures, but also for measuring the colour structure of spectral bands, and it also gives enough

information on the (fractal) features of colours and shades [1, 2]. Let spectral fractal dimension (SFD) be:

$$SFD = \frac{\log \frac{L_{S2}}{L_{S1}}}{\log \frac{S_{S1}}{S_{S2}}} \quad (III)$$

where  $L_{S1}$  and  $L_{S2}$  are measured spectral length on N-dimension colour space,  $S_{S1}$  and  $S_{S2}$  are spectral metrics (spectral resolution of the image).

In practice,  $N = \{1, 3, 4, 6, 8, 10, 12, 32, 60, 79, 126, 224, 242, 254, 488, 498, \dots\}$ :

- N=1 black and white or greyscale image
- N=3 RGB, YCC, HSB, IHS colour space image
- N=4 traditional colour printer CMYK space image, some CMOS sensor
- N=6 photo printer CCpMMpYK space image, Landsat ETM satellite images
- N=32 DAIS7915 VIS-NIR or DAIS7915 SWIP-2 sensors
- N=60 COIS VNIR sensor
- N=79 DAIS7915 all
- N=126 HyMap sensor
- N=254 AISA Hawk sensor
- N=488 AISA Eagle sensor
- N=498 AISA Dual sensor.

In practice the measure of spectral resolution can be equalled with the information theory concept of  $\{S_i=1, \dots, S_i=16, \text{ where } i=1 \text{ or } i=2\}$  bits.

Typical spectral resolution:

- Threshold image - 1 bit
- Greyscale image - 2-16 bits
- Colour image - 8-16 bits/bands.

On this basis, spectral computing is as follows:

- Identify which colour space the digital image is
- Establish spectral histogram in the above space
- Half the image as spectral axis
- Examine valuable pixels in the given N-dimension space part (N-dimension spectral box)
- Save the number of the spectral boxes that contain valuable pixels
- Repeat steps iii-v until one (the shortest) spectral side is only one (bit).

In order to compute dimension (more than two image layers or bands and equal to spectral resolution), the definition of spectral fractal dimension can be applied to the measured data like a function (number of valuable spectral boxes in proportion to the whole number of boxes), computing with simple mathematical average as follows:

$$SFD_{measured} = \frac{n \times \sum_{j=1}^{S-1} \frac{\log(BM_j)}{\log(BT_j)}}{S-1} \quad (IV)$$

where

- $n$  – number of image layers or bands
- $S$  - spectral resolution of the layer, in bits
- $BM_j$  - number of spectral boxes containing valuable pixels in case of  $j$ -bits
- $BT_j$  - total number of possible spectral boxes in case of  $j$ -bits

The number of possible spectral boxes ( $BT_j$ ) in case of  $j$ -bits as follows:

$$BT_j = (2^S)^n \quad (V)$$

### 3. RESULTS

10 parts of field were examined, where 5 different kinds of vegetation could be distinguished: corn, triticosecale, wheat, sunflower and uncultivated land. The examinations included other objects as well, like the road, and the wood band along it which mainly consisted of wattle. Measuring the above introduced SFD structure parameter band by band we were the first to make wavelength-based 16-bit spectral curves 'fingerprints' [6] of these plants and objects (Fig. 4) as well as of the whole images for noise analysis (Fig. 5).

Based on Figure 4 (and the acquired data), plant cultures can definitely be distinguished, and the most adequate spectral bands for certain examinations can be identified. In Figure 5, the curves of the average of the wood, the road and the above mentioned cultivated plants can be seen depending on the number of channels. The above statements can clearly be seen on it. Analysing the features of the curves made of the whole bands, noisy bands can directly be suspected.

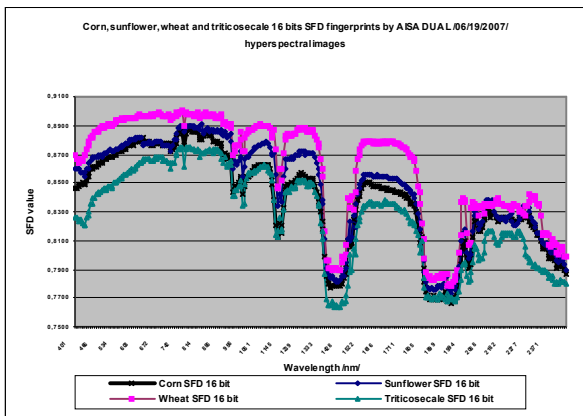


**Figure 4.** Spectral 16-bit SFD 'fingerprints' of corn, sunflower, wheat, and triticosecale (above picture) and of uncultivated land, wood and road (bottom picture) based on AISA Dual data

It was understood that the noise on the whole image (e.g. atmospheric effect) makes colour structure significantly worse, that is, the SFD values significantly and quickly decrease, maybe oscillate.

Such ranges are bands are 116-125, 146-154, 183-204, 284-359. All this can clearly be seen in the images in Fig. 1 and 2, where  $SFD_{2fig} = 0,4451$ ,  $SFD_{1fig} = 0,1622$ . The given ranges are the same as the noisy ranges identified by visual interpretation.

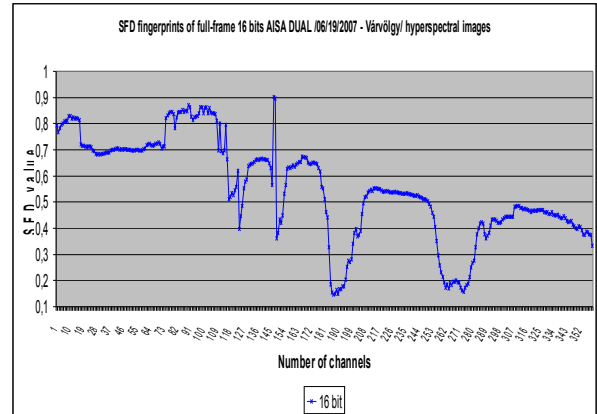


**Figure 5.** 16-bit spectral SFD fingerprint of the whole AISA Dual image (19. June 2007, Várköly) for the identification of noisy bands

In order to identify the inflection point of the red edge in an experimental way, comparing analysis was carried out. For this analysis, the relations suggested by Clevers et al., [4] and Mutanga and Skidmore [10] their SFD and reflectance based calculation connections (Fig 6), Eq. (I) and Eq. (II) were used.

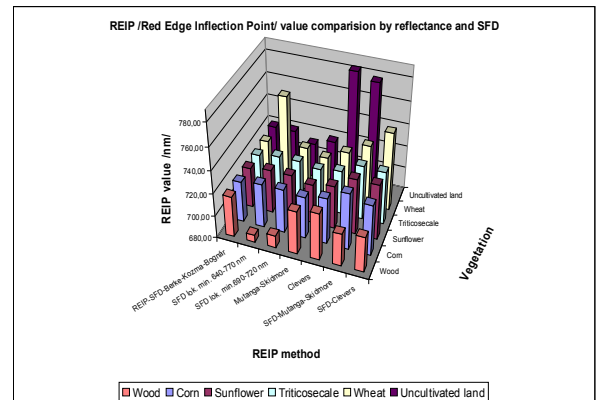


**Figure 6.** Red Edge Inflection Point identification on AISA Dual images using SFD fingerprints and reflectance data

Based on our AISA Dual images we can state that in the case of plant vegetation, in the 640-770 nm and 690-720 nm ranges on SFD based spectra 'fingerprints', red edge inflection point can directly be identified by searching a local minimum (Fig 7).

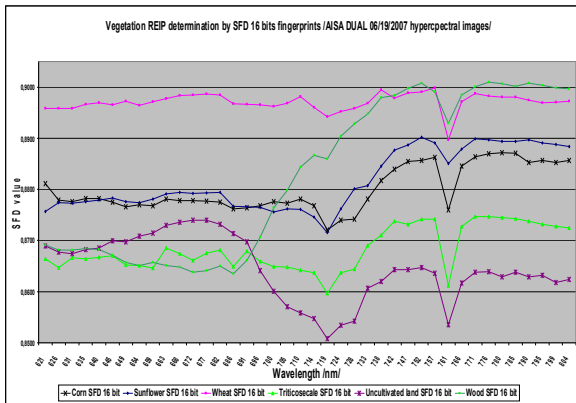


**Figure 7.** Identification of red edge inflection point on 16-bit SFD curves of AISA Dual images based on local minimums

It is therefore suggested that on SFD curves, red edge inflection point be according to the following connection (Table 2.) [7]:

$$\lambda_{re} = 690 + \{SFD_{AVERAGE} (690-720)\} * 30 \quad (VI)$$

**Table 2.** Measured and calculated data for red edge inflection point identification in nanometer, based on 16-bit SFD curves and reflectance data of AISA Dual images

	<b>REIP-SFD-Berke-Kozma-Bognár</b>	<b>Mutanga-Skidmore</b>	<b>Clevers</b>
<b>Corn</b>	716,29	717,19	720,89
<b>Sunflower</b>	716,26	714,80	718,49
<b>Wheat</b>	716,89	714,41	723,78
<b>Triticosecale</b>	715,93	716,18	718,98
<b>Uncultivated land</b>	715,75	711,10	717,36
<b>Wood</b>	716,36	718,51	721,88

Though the SFD based measurements we described make different terrain and spectral resolution image data procession possible, the correspondence we suggested under Eq. (VI) is useable with SFD values measured in hyperspectral data, but not in multispectral ones.

#### 4. CONCLUSION

The SFD-based data processing method we have developed is directly built on calculations on the structure of image data from remote sensing devices, does not necessarily require the application of complementary aerial or terrain radiation sensors, still it gives well-applicable information in several cases. SFD-based structure data are less sensitive to terrain, atmospheric or other correction factors, as they are based on logarithmic calculations. Fingerprints have been developed that, besides terrain identification, can also be calculated using only image information, thus avoiding disadvantages deriving from the lack or inaccuracy of the above mentioned corrections. SFD spectral curves have been created, with the help of which given surface shapes can be described, characterised, identified and mapped similarly to reflectance

curves. When creating a REIP index, SFD spectral curve might even give an easier calculation result.

For the identification of red edge inflection point, an experimental correspondence is suggested Eq. (VI), which, similarly to the presently used experimental correspondence, gives an easily calculable result with the use of SFD spectral curves.

#### 5. REFERENCES

- [1] J. Berke, "Measuring of Spectral Fractal Dimension", **Advances in Systems, Computing Sciences and Software Engineering**, Springer, 2006, pp. 397-402., ISBN 10 1-4020-5262-6.
- [2] J. Berke, "Measuring of Spectral Fractal Dimension", **Journal of New Mathematics and Natural Computation**, 3/3: 409-418, 2007, ISSN 1793-0057.
- [3] N. H. Broge, J. V. Mortensen, "Deriving green crop area index and canopy chlorophyll density of winter wheat from spectral reflectance data", **Remote Sensing of Environment**, 80. 45–57, 2002.
- [4] J.G.P.W. Clevers, S.M. De Jong, G.F. Epema, F.D Van Der Meer, W.H. Bakker, A.K Skidmore, K.H. Scholte, "Derivation of the red edge index using the MERIS standard band setting", **International Journal of Remote Sensing**, 23 (16), 3169–3184, 2002.
- [5] EU Council, "149/2003/EK internal regulation".
- [6] V. Kozma-Bognár, J. Berke, „New Applied Techniques in Evaluation of Hyperspectral Data”, **Georgikon for Agriculture**, Number 1, Volume 12, 2009, ISSN: 0239 1260.
- [7] V. Kozma-Bognár, J. Berke, „New Evaluation Techniques of Hyperspectral Data”, **The 13th World Multi-Conference on Systemics, Cybernetics and Informatics**, Orlando, Florida, USA, 2009, ISBN: 978-1-934272-74-9.
- [8] V. Kozma-Bognár, P. Hermann, K. Bencze, J. Berke, J. Busznyák, „Possibilities of an Interactive Report on Terrain Measurement”, **Journal of Applied Multimedia**, No. 2/III/2008, pp. 33-43., ISSN 1789-6967.
- [9] B. B. Mandelbrot, **The fractal geometry of nature**, W.H. Freeman and Company, New York. 1983.
- [10] O. Mutanga, A. K. Skidmore, "Integrating imaging spectroscopy and neural networks to map grass quality in the Kruger National Park, South Africa", **Remote Sensing of Environment**, 90. 104–115, 2004.
- [11] H-O Peitgen, D. Saupe, **The Science of fractal images**, Springer-Verlag, New York, 1988.
- [12] F. F. Sabin, **Remote Sensing. Principles and Interpretation**, W. H. Freeman and Co. Los Angeles, 1987, ISBN 0-7167-1793-X.
- [13] SFD official website: [www.digkep.hu/sfd/index.htm](http://www.digkep.hu/sfd/index.htm)
- [14] R. A Schowengerdt, **Remote Sensing Models and Methods for Image Processing**, Elsevier, 2007, ISBN 13: 978-0-12-369407-2.
- [15] P. K. Varshney, M. K. Arora, **Advanced Image Processing Techniques for Remotely Sensed Hyperspectral Data**, Springer-Verlag, New York, 2004.